WOOD RESEARCH
65 (5): 2020
757-770
doi.org/10.37763/wr.1336-4561/65.5.757770

ALTERATIONS IN THE ANATOMY AND CHEMICAL STRUCTURE OF ARCHAEOLOGICAL WOOD FROM A TOMB OF NORTHERN CHINA DUE TO DIFFERENT FUNGAL ROTS

Yihang Zhou, Kai Wang, Xueqi Chen, Dongbo Hu
Peking University
P.R. China

(Received January 2020)

ABSTRACT

This paper aims to identify the decay types and investigate the chemical alterations in the three types of fungal decayed archaeological wood from Dongshan Han Tomb M6 (ca. 200-100 B.C.) in Taiyuan City, China. Microscopy, FT-IR, ^{13}C NMR and XPS were adopted to reveal the features of the samples. The results show that from the microscopic and chemical perspectives, these samples are consistent with the characteristics of brown-rot, white-rot and soft-rot. However, all the samples show the accumulation of carboxylic acids or carboxylate salts from extensive oxidation of lignin, which were not observed in artificial fungal decayed wood. Moreover, different fungal decay types and pH values of the samples corresponding to the alternative forms of carboxylic acid or carboxylate salt are considered to be influenced by combined factors, such as the position in the tomb, groundwater level, moisture content, oxygen availability, etc. This study may provide a reference for the deterioration and conservation of fungal decayed wooden artifacts in the tomb of northern China where alkaline loess is the main soil type.

KEYWORDS: Archaeological wood, wood decay, microscopy, FT-IR, XPS, ^{13}C NMR.

INTRODUCTION

Wood is an excellent natural material for construction and making tools due to its outstanding mechanical properties and availability. Our ancestors once made countless wooden crafts, which unfortunately, were degraded and sometimes even fully decomposed as a comprehensive result of bacteria, fungi, shipworms, insects, fire, physical abrasions, etc. Bacterial decays, especially erosion bacteria and tunneling bacteria, are the main factors causing the deconstruction in most

waterlogged archaeological wood (Björdal et al. 1999, Björdal 2012, Blanchette 2000). But bacterial decay is considered to be relatively slow in comparison to fungal ones (Klaassen 2014), explaining most of well-preserved archaeological wood was excavated in waterlogged conditions where fungal decays were suppressed, e.g. famous warships Mary Rose (Sandstrom et al. 2005) and Vasa (Hocker 2006). However, when the climate conditions are favorable to wood decay fungi, the decomposition would be much more rapid and detrimental, probably causing the absence of wooden findings in the tombs located in semiarid/semihumid regions. This might be one reason explaining the lack of studies on fungal decay in archaeological wood in northern China. Three main types of wood fungal decay are commonly recognized as brown rot, white rot and soft rot, each with its unique microscopic morphological characteristics (Schwarze et al. 2007). Wood fungal decay has also been studied by various chemical analytical methods, e.g. Fourier transform infrared spectroscopy (Gelbrich et al. 2012, Pandey et al. 2003), X-ray photoelectron spectroscopy (Pandey et al. 2003, Xu et al. 2013), Py-GC/MS (R10 et al. 2002, R10 et al. 2002, Vinciguerra et al. 2007) and thermogravimetry (Romagnoli et al. 2018), to acquire different aspects of chemical features. Generally speaking, the degradation of archaeological wood in aerated environments is more complex than that from anoxic waterlogged environment, which can be caused by all three types of fungi and result in poor structure preservation (Tamburini et al. 2017).

To the best of our knowledge, there has been no reports on a single archaeological unit where all three types of wood fungal decays happened, or at least noticed. But here in this paper, such materials were acquired from a tomb of Western Han Dynasty (ca. 200-100 B.C.), named as Dongshan Han Tomb M6 and excavated in 2018 in Taiyuan City, Shanxi, China. This suggests that even within a close distance there might have been variations in micro-environment resulting in different fungal decays in archaeological wood. Moreover, wooden artifacts haven't been paid adequate attentions during tomb excavations in northern China due to their poor preservation. But in this tomb, Shanxi's first batch of wooden slips (main writing materials in pre-paper times in China) recording ancient medical literatures were found, which adds more significance to the understanding of their deterioration causes. Hence, it is a great opportunity to investigate the chemical alterations of the archaeological wood with different decay features and further understand wood decay in tomb environment of northern China. To acquire the morphological, elemental and structural profiles of the wooden slips and the coffin, their current statuses are analyzed by microscopy, X-ray photoelectron spectroscopy (XPS), Fourier transform infrared spectroscopy (FT-IR), and solid state ^{13}C nuclear magnetic resonance (^{13}C NMR).

MATERIALS AND METHODS

Materials

Dongshan Han Tomb M6 is an accessory noble tomb to a feudatory king's tomb of Western Han Dynasty in Shanxi. It was integrally moved and excavated in laboratory in 2018-2019. The wooden coffin boards (identified as *Pinus* sp., possibly local prevailing *Pinus tabuliformis* Carr.) showed two types of deterioration similar to brown-rot and white-rot decays respectively (confirmed in the microscopic results). One type was easily broken into blocks in dark brown color (Fig. 1a) while the other was more fibrous with pale yellow color inside (Fig. 1b) and possibly related to white pocket rot phenomenon (Blanchette 1980, Otjen et al. 1982). Both types of decayed wood from the same cover board of the coffin were sampled. Soft-rot decay was noticed on the wooden slips (Fig. 1c, identified as possibly *Picea* sp.) in dark color located at the bottom of the tomb and closed to the foot end, which was also selected as samples. Sound sapwood

of *Pinus* sp. was used as reference in chemical analysis because sapwood within the family Pinaceae is basically the same with respect to the main constituents while additional components in heartwood may vary.

Fig. 1: Two types of decayed wood of coffin (a, b) and wooden slips (c).

Observation under microscope

In the typical protocol of wood microscopic sections, the samples were first hydrated by soaking in distilled water and then immersed in melted polyethylene glycol (PEG 4000) at 60°C overnight. For brittle samples, they were infiltrated by n-butyl methacrylate with 1% AIBN (2,2-azobisisobutyronitrile) and heated at 60°C overnight, resulting in cured resin. Thereafter, the embedded wood samples were sectioned into 10-20 µm using Thermo Scientific HM 450 microtome. The sections were mounted in water or neutral resin medium, inspected under optical microscope (Leica DM4500P). For microscopic sections with typical white rot features, Safranine and Astra blue were used to differentiate the de-lignified areas (Schwarze et al. 1998, Srebotnik et al. 1994). The wood section was first stained by Safranine (1% in ethanol) for 3 min, then by Astra blue (1% water solution) for 10 seconds, and finally washed by deionized water. Also, scanning electron microscope (SEM, Hitachi TM3030) was used to observe the samples under low vacuum mode with 15kV working voltage when optical microscope failed to reveal the necessary features due to magnification limits. The sample's section was prepared by a brittle rupture so that no physical friction might cause unexpected alteration in the appearance.

FT-IR analysis

Chemical compositions of grinded wood samples were determined by attenuated total reflectance - Fourier transform infrared spectroscopy (Thermo Fisher Nicolet IS50) with a range from 4000 cm^{-1} to 400 cm^{-1}. The FT-IR spectra were analyzed by Peakfit v4.12 software for deconvolution.

XPS analysis

The grinded wood samples were tested by X-ray photoelectron spectrometer (AXIS Supra from Kratos Analytical Ltd.) using mono Al source (150 W) with a minimum analyzed area of 15 µm × 15 µm to acquire the oxidation states of the remaining components. For acquiring survey spectra, the pass energy was 160 eV, energy steps 1.000 eV and total acquiring time 55.550 s (50.0 ms x 1 x 1111). For C 1 s spectra, the pass energy was 40 eV, energy steps 0.100 eV and total acquiring time 40.200 s (200.0 ms x 1 x 201). The XPS spectra were analyzed by CASAXPS software for deconvolution.

Solid state CP/MAS ^{13}C NMR spectroscopy

The CP/MAS ^{13}C NMR spectra of grinded wood samples were obtained using 400 MHz WB Solid-State NMR Spectrometer (Bruker AVANCE III) equipped with WVT 4 mm cross

polarization and magic angle spinning (CP/MAS) double resonance probe head. The detailed testing parameters were selected according to the literature (Popescu et al. 2009).

PH measurement

The pH values of the samples were measured by METTLER TOLEDO S20 SevenEasy. Prior to the measurement, the pH-meter was calibrated by standard solutions of potassium hydrogen phthalate (pH = 4.01), phosphate buffer (pH = 6.86) and borate buffer (pH = 9.18). The wood powder suspension was prepared by mixing 1 g of the sample with 100 ml distilled water, heating at 50°C for 1 h and cooling down to room temperature. The soil suspension was prepared by mixing 10 g soil and 10 ml distilled water. The measurements of each kind were taken on three replicate specimens.

RESULTS

Determination of decay type by microscopy

Three types of decayed wood are shown in Fig. 2., Although hypha presents in the lumen and rays (red arrows) and clefts (blue arrows) in the secondary walls (Fig. 2a,c), most of the cell wall structures are intact morphologically. These clefts are shuttle-shaped with varied lengths longitudinally from approximately 5 to 30 μm (Fig. 2c). Similar clefts were also observed in oak wood incubated with brown-rot fungus *Laetiporus sulphureus* (Schwarze et al. 2007). Under cross polarized light, the birefringence of the S3 and S2 layers of secondary walls has completely disappeared, indicating most of the crystalline cellulose has been decomposed. Only S1 layers in a limited number of cell walls remain weak birefringence. On the basis of selective cellulose degradation, clefts and largely retained secondary wall, the wood sample in Fig. 2a,b,c was typically deteriorated by brown-rot fungi.

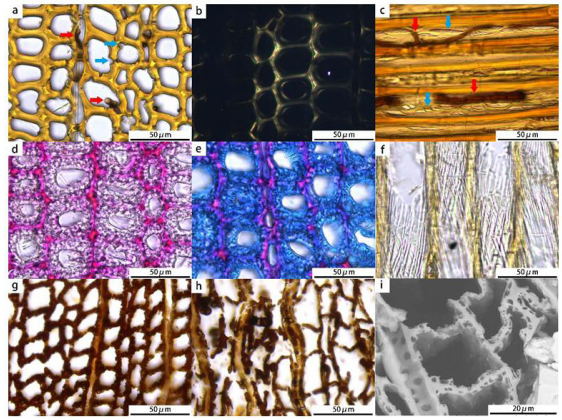

Fig. 2: Micrographs of (a) brown-rot coffin wood transection, (b) transection under cross polarized light, (c) radial section, (d) white-rot coffin wood transection stained by safranine, (e) transection stained by safranine and astra blue, (f) tangential section, (g) transection of wooden slips showing eroded cell walls, (e) highly deteriorated part with spores, and (f) eroded cell wall with longitudinal cavities under SEM showing soft-rot features.

The wood section in Fig. 2d was stained by safranine where all the middle lamella and cell corners turned into red, while the porous secondary walls (mainly S2 layers) were less stained. After stained by astra blue which only stains cellulose in the absence of lignin (Schwarze et al. 1998, Srebotnik et al. 1994), the secondary walls turned into blue (in Fig. 2e), suggesting selective delignification had taken place in the secondary walls, which is one of the typical degradation mode caused by white-rot fungi of the delignification type (Blanchette 2000, Schwarze et al. 2007). In tangential section (Fig. 2f), separated micro-fibrils in the original micro-fibril angle were exposed since lignin had been completely decomposed in S_2 layers.

In the wooden slips, the secondary walls were severely eroded, causing the reduction of thickness (Fig. 2g,h). Widespread cavities located in secondary wall (Fig. 2i) match the typical feature of soft-rot decay (Blanchette 2000, Schwarze et al. 2007). As a matter of fact, various microbes in soil, insects as well as abiotic hydrolysis and oxidation could have influenced the decay features of the samples. However, it is reasonable to classify them as the corresponding fungal decay types because of their pronounced morphological features.

FT-IR results

After confirming the decay types of the samples, it is now possible to compare their chemical alteration related to the determined decay types. The FT-IR spectra are shown in Fig. 3.

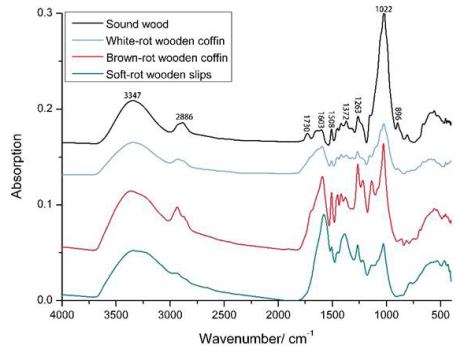

Fig. 3: FT-IR spectra of analyzed wood samples.

The spectrum of the white-rot wooden coffin is most similar to that of sound wood as a result of preservation of cellulose demonstrated by a weak but clear absorption at 896 cm^{-1} assigned to C-H deformation in cellulose and other strong cellulose-related absorptions such as 1372 cm^{-1} (C-H plane deformation in cellulose and hemicellulose) and 1022 cm^{-1} (mainly C-O stretching in cellulose). However, for brown-rot and soft-rot samples, preferential degradation of cellulose has caused a complete loss of absorption at 896 cm^{-1} in FT-IR spectra. Therefore, their 1508 cm^{-1}/1022 cm^{-1} intensity ratios are much higher than those in sound wood and the white-rot wood sample. It is hard to interpret the presence of hemicellulose in FT-IR spectra as most of its absorptions are the same as cellulose except the absorption at 1730 cm^{-1} assigned to acetyl group from hemicellulose. After deconvolution, the carbonyl-related absorptions become clearer (Fig. 4). The absence of absorption at 1730 cm^{-1} in all spectra of decayed wood samples indicates a complete loss of hemicellulose as it is considered to be degraded in the early stage of all types of fungal decays (Eriksson et al. 1990). Interestingly, new peaks appear at 1757-1749 cm^{-1} and 1705-1701 cm^{-1} in both white-rot and brown-rot samples, which suggests they are probably assigned to similar molecular structures from degradation. As the relative intensities of carboxylic

group absorptions to that of aromatic ring absorption from lignin (around 1600 cm^{-1}) are comparable in both Fig. 4b and Fig. 4c, the newly formed carboxylic groups should be resulted from the oxidation of lignin rather than cellulose. Brown-rot fungi, however, can alter the structure of lignin to a very limited extent and only demethylation shall presents (Eriksson et al. 1990, Ohkoshi et al. 1999). Also, these two newly formed carbonyl absorptions were not observed in the FT-IR studies of artificially decayed wood inoculated with brown-rot and white-rot fungi (Durmaz et al. 2016, Li et al. 2011, Pandey et al. 2003, Rudakiya et al. 2019, Xu et al. 2013). Therefore, the formation of new carboxylic acids at 1705-1701 cm^{-1} and 1757-1749 cm^{-1} requires more information, possibly related to the specific burial environment, to be explained.

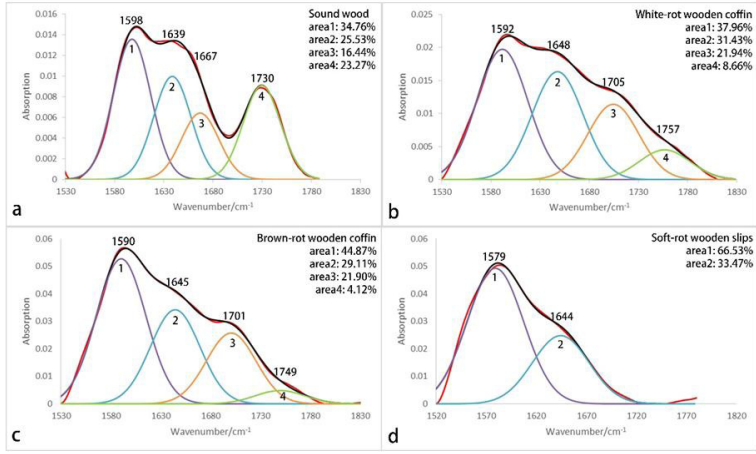

Fig. 4: Deconvolution of FT-IR spectra concerning carbonyl groups.

More proportions of peak 4 in Fig. 4b than those in Fig. 4c may be the result of previous delignification by white-rot fungi and it making the remaining lignin more accessible and reactive to the degradation factors. As for the spectrum of the soft-rot sample in Fig. 4d, there is no absorption bands at around 1701 cm^{-1} and 1749 cm^{-1}. But it is doubtful that the absence of these bands would be attributed to very limited oxidation of lignin. The absorption at 1508 cm^{-1} decreased dramatically and the band at around 1590-1603 cm^{-1} has shifted to 1579 cm^{-1}, suggesting the decomposition or structural alteration of lignin. Additionally, the band at 1372 cm^{-1} normally assigned to C-H plane deformation in cellulose and hemicellulose increases and shifts to 1387 cm^{-1}. These two increased absorptions at 1579 cm^{-1} and 1387 cm^{-1} are consistent to asymmetric and symmetric stretching vibrations of carboxylate groups. Thus, XPS and solid state ^{13}C NMR were used to confirm the presence of carboxylate and further analyzed the degradation outcomes.

Solid state CP/MAS ^{13}C NMR results

From the CP/MAS ^{13}C NMR spectra in Fig. 5 and the main assignments of the signals (Melkior et al. 2017, also listed in Tab. 1), similar conclusions can be drawn as the FT-IR results with respect to the wood constituents. For sound wood, the holocellulose-related signals are much stronger than lignin-related ones. Therefore, the spectrum of the delignified white-rot sample was barely altered compared to that of sound wood except the absence of signal 15 related

to hemicellulose and the decrease of signal 2 and 10 related to lignin. All the strong signals from 7 to 12 in the spectrum of white-rot sample shows the high content of cellulose and the signal 8 assigned to crystalline cellulose suggests the well-preserved cellulose and its crystalline structure. The amorphous cellulose, however, seems to be degraded, which is judged by the relative height of signal 8 to 9 compared to that of the sound wood. Differently, lignin-originated signals from 2 to 6 and 14 are much stronger and cellulose-originated signals are weaker in the spectra of the brown-rot sample and the soft-rot sample. The crystalline cellulose in the brown-rot and soft-rot samples was progressively degraded by fungi as the signal 8 dramatically decreased. In addition, the pronounced signal 1 referring to carboxyl groups in the spectrum of the soft-rot sample confirms the presence of carboxylate salts as speculated from the FT-IR results.

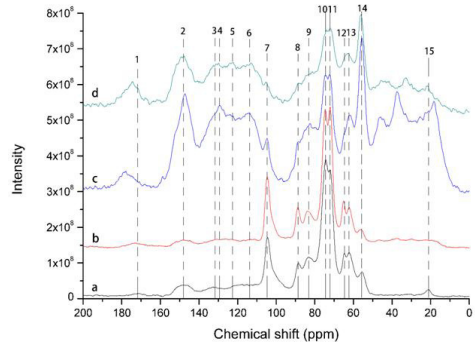

Fig. 5: CP/MAS ^{13}C NMR spectra of (a) sound wood, (b)the white-rot sample, (c)the brown-rot sample, and (d) the soft-rot sample.

Tab. 1: Main assignments of CP/MAS 13C NMR spectra of the samples.

Signal number	Chemical shift (ppm)	Main assignments
1	171.5	Acetyl groups in hemicellulose
2	147.3	G3, G4 in lignin
3	132.8	Non-esterified G1 in lignin
4	129.1	Esterified G1 in lignin
5	123.4	G6 in lignin
6	113.3	G5, G2 in lignin
7	104.6	C1 in cellulose
8	88.8	C4 in crystalline cellulose
9	83.6	C4 in amorphous cellulose
10	74.7	Cα in lignin; C2, C3, C5 in holocellulose
11	72.1	C2, C3, C5 in holocellulose
12	65.1	C6 in holocellulose
13	62.2	Cγ in lignin
14	56.1	OCH_3 in lignin
15	21.0	Acetyl groups in hemicellulose

(G refers to guaiacyl, aromatic unit with only one methoxyl. G1- G6 refer to C atoms in guaiacyl ring where G1 is the one bonded to akyl side chain and Cα- Cγ refer to those in akyl side chain.)

XPS results

To further analyze the oxidative status of the wood components, XPS analysis were used. The quantified elemental data are shown in Tab. 2, and the XPS scans of C 1s region are shown in Fig. 6. The assignment of deconvoluted peaks C 1s for lignocellulosic materials corresponding to four types of carbon atoms (C1-C4) is well established (Kamdem et al. 2001, Liu et al. 1998, Nzokou et al. 2010) and listed in Tab. 3. Due to decomposition or losses of hemicellulose and cellulose, all the samples show decrease in O/C ratios in Tab. 2.

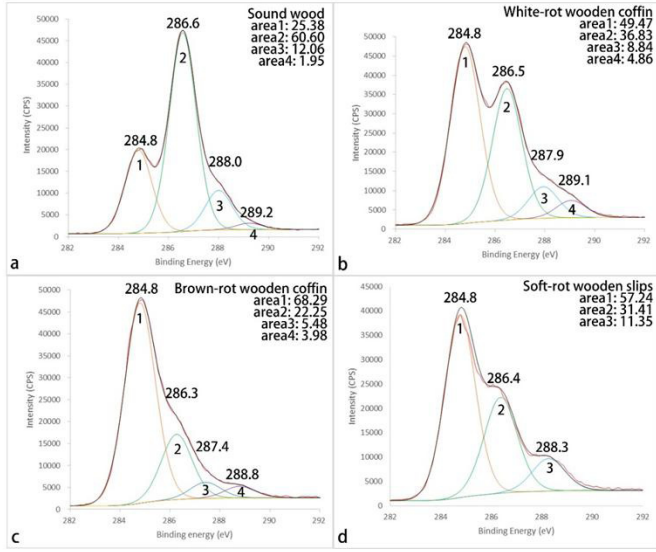

Fig. 6: XPS scan of C 1s region.

Tab. 2: Quantified XPS data of the samples.

Sample	C	O	N	Si	Ca	O/C ratio
Sound wood	65.67	34.33	/	/	/	0.523
White-rot wooden coffin	71.78	26.48	0.50	0.41	0.84	0.369
Brown-rot wooden coffin	79.90	18.13	0.70	0.49	0.77	0.227
Soft-rot wooden slips	67.24	26.53	1.99	1.74	2.50	0.395

Tab. 3: Peak assignment of C 1s region of the samples.

Peak	Binding energy (eV)	Corresponding chemical bond
C1	284.8	C-C or C-H
C2	286.3-286.6	C-O
C3	287.4-288.0	C=O or O-C-O
C3*	288.3	O=C-O$^-$
C4	288.8-289.2	O=C-OR

(C3*only appears in the results of wooden slips).

For white-rot wooden coffin, the selective delignification and the remaining cellulose contributed to the relatively higher O/C ratio and larger area of peak C2 in Fig. 6b compared to the brown-rot type. The O/C ratio and peak C2 in Fig. 6c of the brown-rot sample are unsurprisingly the lowest since most of the carbohydrates (both cellulose and hemicellulose) were degraded, which is consistent to FT-IR results and NMR results. The O/C ratio of soft-rot sample is the highest among the decayed types. However, from the FT-IR and NMR results, cellulose in the soft-rot sample has been decomposed to a large extent. The main reason of the increased O/C ratio would be attributed to further oxidation of lignin, which is also demonstrated by larger peak area of C3 in Fig. 6d.

Moreover, the peak C4 representing carboxyl groups cannot be detected in XPS results of the soft-rot sample in Fig. 6d, which is consistent to the absence of absorptions over 1700 cm^{-1} in FT-IR spectrum. Both XPS and FT-IR results demonstrate the absence of carboxylic acids while the binding energy of peak C3 in Fig. 6d shifted from normally 288.0 eV (or lower) to 288.3 eV, consistent with the binding energy of carboxylate salts (Hammond et al. 1981). Hence, all the carboxylic acids in the wooden slips turned into salts, indicating a unique preservation condition that neutralized the newly formed acids. These salts were probably formed from the $CaCO^3$ in the local loess based on higher content of calcium in Tab. 2 with no other metal detected. In addition, higher content of nitrogen (Tab. 2s) in the wooden slips might as well favor the growth of fungi and enzyme production, which is possibly resulted from its lower position closed to the completely rotted body of the tomb.

DISCUSSION

One of the unsolved problems concerning deterioration of archaeological wood buried underground is to what extent it was caused by biochemical processes and abiotic chemical reactions. Presumably, no wood can be continuously degraded by fungi for approximately 2000 years and still preserved. The fungal decay processes were likely to happen during the first few years after the burial or after certain incident such as the excavation when the tomb's environmental conditions dramatically changed. This assumption allows us to further understand the difference between the fungal decay features and abiotic decay ones. For instance, cellulose, especially crystalline part, was largely preserved in the white-rot sample, suggesting abiotic hydrolysis of crystalline cellulose was extremely limited in this tomb environment. Also, cellulose in archaeological wood without evident microbial decay appeared to be well-preserved in a previous finding from southern China (Zhou et al. 2018). On the contrary, the cellulose in the brown-rot sample was largely degraded and mainly lignin remains. From the above results, the analyzed samples generally fit the fungal decay features morphologically and chemically. But the carboxylic acids in both brown-rot and white-rot samples and the carboxylate salts in the soft-rot sample were not observed in previous research on wood fungal decay (Durmaz et al. 2016, Li et al. 2011, Pandey et al. 2003, Rudakiya et al. 2019, Xu et al. 2013). The presence of fungal decays suggests the environment in the tomb was oxic, or at least meets the requirement of aerobic fungi. Therefore, a continuous oxidation of lignin probably caused the accumulation of carboxylic acids in the samples.

The conversion from carboxylate acid to its salt form was, of course, directly determined by the pH values of the sample and its surroundings. The white-rot and brown-rot samples are both acidic (pH 4.67 and pH 6.02 respectively), while the soft-rot sample is slightly alkaline (pH 7.26), which is also indicated from their chemical profiles. Moreover, only the acids in the

soft-rot sample were evidently neutralized by $CaCO_3$ from loess, while those in the other samples were not. The brown-rot and white-rot samples were collected from the cover board of the coffin, while the soft-rot sample was located at the very bottom of the coffin. Thus, one possible explanation is that the groundwater level did not reach the top of the coffin but sometimes exceeded the bottom because water provided the necessary medium for ion exchange. The fact that soft-rot requires very little oxygen and prefers high moisture content (Nelson et al. 1995) also supports this hypothesis. Additionally, Brown-rot fungi and white-rot fungi reach optimum growth at pH values of 5-6, the total growth range between 2.5 to 9, while soft-rot fungi tolerant alkaline substrates at pH values up to 11 (Zabel et al. 1992). As the pH value of the soil in the tomb is 8.33 due to the presence of $CaCO_3$ in loess, the pH conditions do not actually favor the growth of fungi, especially where ion exchange was more frequent. Although wood itself is acidic and fungi are capable of excreting acids to adjust the pH value of their surroundings to their own requirements (Unger et al. 2001), the wooden slips lying at the bottom of the tomb was still more suitable for soft-rot fungi. Therefore, the presence of three different types of fungal decay in the same tomb and their chemical features are comprehensively influenced by the surrounding pH values, the groundwater levels, oxygen availability, etc.

From the perspective of conservation of artifacts, relative high contents of carboxylic acids or carboxylate salts should be taken into consideration when selecting conservation methods for fungal decayed the wooden artifacts.

CONCLUSIONS

The overall morphological and chemical alterations of the samples decayed by brown-rot, white-rot and soft-rot respectively are consistent with the features reported in previous work. However, the extensive oxidation of lignin and formation of carboxylic acids or carboxylate salts in these samples are the major points that distinguish them from other fungal decay cases. Moreover, various factors including $CaCO_3$ from local loess, groundwater level, oxygen availability, etc., might result in the different fungal decay types and special chemical features (e.g. accumulation of carboxylic acids and carboxylate salts) occurred in the wood of this tomb from northern China.

ACKNOWLEDGEMENT

This work was supported by the National Social Science Foundation of China (Grant No. 19CKG032).

REFERENCES

1. Björdal, C.G., Nilsson, T., Daniel, G., 1999: Microbial decay of waterlogged archaeological wood found in Sweden applicable to archaeology and conservation. International Biodeterioration & Biodegradation 43: 63-73.
2. Björdal, C.G., 2012: Microbial degradation of waterlogged archaeological wood. Journal of Cultural Heritage 13: S118-S122.
3. Blanchette, R.A., 1980: Wood decomposition by *Phellinus (Fomes) pini*: a scanning electron microscopy study. Canadian Journal of Botany 58(13): 1496-1503.

4. Blanchette, R.A., 2000: A review of microbial deterioration found in archaeological wood from different environments. International Biodeterioration & Biodegradation 46: 189-204.
5. Durmaz, S., Özgenç, O., Boyacı, I.H., Yıldız, U.C., Erişir, E., 2016: Examination of the chemical changes in spruce wood degraded by brown-rot fungi using FT-IR and FT-Raman spectroscopy. Vibrational Spectroscopy 85:202-207.
6. Eriksson, K.E.L., Blanchette, R.A., Ander, P., 1990: Microbial and enzymatic degradation of wood and wood components. Springer. Heidelberg, Pp 20-56.
7. Gelbrich, J., Mai, C., Militz. H., 2012: Evaluation of bacterial wood degradation by Fourier transform infrared (FTIR) measurements. Journal of Cultural Heritage 13: S135-S138.
8. Hammond, J.S., Holubka, J.W., Devries, J.E., Dickie, R.A., 1981: The application of x-ray photo-electron spectroscopy to a study of interfacial composition in corrosion-induced paint de-adhesion. Corrosion Science 21: 239-253.
9. Hocker, E., 2006: From the micro- to the macro-: managing the conservation of the warship, vasa. Macromolecule Symposium 238(1): 16-21.
10. Kamdem, D.P., Zhang, J., Adnot, A., 2001: Identification of cupric and cuprous copper in copper naphthenate-treated wood by X-ray photoelectron spectroscopy. Holzforschung 55: 16-20.
11. Klaassen, R.K.W.M., 2014: Speed of bacterial decay in waterlogged wood in soil and open water. International Biodeterioration & Biodegradation 86: 129-135.
12. Li, G.Y., Huang, L.H., Hse, C.Y., Qin, T.F., 2011: Chemical compositions, infrared spectroscopy, and x-ray diffractometry study on brown-rotted woods. Carbohydrate Polymers 85: 560-564.
13. Liu, F.P., Rials, T.G., Simonsen, J., 1998: Relationship of wood surface energy to surface composition. Langmuir 14: 536-541.
14. Melkior, T., Barthomeuf, C., Bardet. M., 2017: Inputs of solid-state nmr to evaluate and compare thermal reactivity of pine and beech woods under torrefaction conditions and modified atmosphere. Fuel 187: 250-260.
15. Nelson, B.C., Goñi, M.A., Hedges, J.I., Blanchette, R.A., 1995: Soft-rot fungal degradation of lignin in 2700 year old archaeological woods. Holzforschung 49: 1-10.
16. Nzokou, P., Kamdem, D.P., 2010: X-ray photoelectron spectroscopy study of red oak- (*Quercus rubra*), black cherry - (*Prunus serotina*) and red pine - (*Pinus resinosa*) extracted wood surfaces. Surface and Interface Analysis 37: 689-694.
17. Ohkoshi, M., Kato, A., Suzuki, K., Hayashi, N., Ishihara, M., 1999: Characterization of acetylated wood decayed by brown-rot and white-rot fungi. Journal of Wood Science 45: 69-75.
18. Otjen, L., Blanchette, R.A., 1982: Patterns of decay caused by *Inonotus Dryophilus* (Aphyllophorales: Hymenochaetaceae), a white-pocket rot fungus of oaks. Canadian Journal of Botany 60: 2770-2779.
19. Pandey, K.K., Pitman, A.J., 2003: FTIR studies of the changes in wood chemistry following decay by brown-rot and white-rot fungi. International Biodeterioration & Biodegradation 52: 151-160.
20. Popescu, C.M., Tibirna, C.M., Vasile. C., 2009: XPS characterization of naturally aged wood. Applied Surface Science 256: 1355-1360.
21. Popescu, C.M., Larsson, P.T., Vasile. C., 2011: Carbon-13 CP/MAS solid state NMR and X-ray diffraction spectroscopy studies on lime wood decayed by *Chaetomium globosum*. Carbohydrate Polymers 83:808-812.

22. Rıo, J.D., Speranza, M., Gutiérrez, A., Martınez, M.J., Martınez, A.T., 2002: Lignin attack during eucalypt wood decay by selected basidiomycetes: a Py-GC/MS study. Journal of Analytical and Applied Pyrolysis 64: 421-431.
23. Romagnoli, M., Galotta, G., Antonelli, F., Sidoti, G., Humar, M., Kržišnike, D., Čufare, K., Petriaggi, B.D., 2018: Micro-morphological, physical and thermogravimetric analyses of waterlogged archaeological wood from the prehistoric village of Gran Carro (lake Bolsena-Italy). Journal of Cultural Heritage 33: 30-38.
24. Rudakiya, D.M., Gupte, A., 2019: Assessment of white rot fungus mediated hardwood degradation by FTIR spectroscopy and multivariate analysis. Journal of Microbiological Methods 157: 123-130.
25. Sandstrom, M., Jalilehvand, F., Damian, E., Fors, Y., Gelius, U., Jones, M., Salome, M., 2005: Sulfur accumulation in the timbers of King Henry VIII's warship Mary Rose: a pathway in the sulfur cycle of conservation concern. Proceedings of the National Academy of Science USA 102: 14165-14170.
26. Schwarze, F.W.M.R., Engels, J., 1998: Cavity formation and the exposure of peculiar structures in the secondary wall (S2) of tracheids and fibres by wood degrading basidiomycetes. Holzforschung 52: 117-123.
27. Schwarze, F.W.M.R., 2007: Wood decay under the microscope. Fungal Biology Review 21: 133-170.
28. Srebotnik, E., Messner, K., 1994: A simple method that uses differential staining and light microscopy to assess the selectivity of wood delignification by white rot fungi. Applied and Environmental Microbiology 60: 1383-1386.
29. Tamburini, D., Łucejko, J.J., Zborowska, M., Modugno, F., Prądzyński, W., Colombini, M.P., 2015: Archaeological wood degradation at the site of Biskupin (Poland): wet chemical analysis and evaluation of specific Py-GC/MS profiles. Journal of Analytical and Applied Pyrolysis 115: 7-15.
30. Tamburini, D., Łucejko, J.J., Pizzo, B., Mohammed, Y., Sloggett, R., Colombini. M.P., 2017: A critical evaluation of the degradation state of dry archaeological wood from Egypt by SEM, ATR-FTIR, wet chemical analysis and Py(HMDS)-GC-MS. Polymer Degradation and Stability 146: 140-154.
31. Unger, A., Schniewind, A.P., Unger, W., 2001: Conservation of wood artifacts a handbook. Springer. Heidelberg, 98 pp.
32. Vinciguerra, V., Napoli, A., Bistoni, A., Petrucci, G., Sgherzi, R., 2007: Wood decay characterization of a naturally infected London plane-tree in urban environment using Py-GC/MS. Journal of Analytical and Applied Pyrolysis 78: 228-231.
33. Xu, G. Wang, L., Liu, J., Wu, J., 2013: FTIR and XPS analysis of the changes in bamboo chemical structure decayed by white-rot and brown-rot fungi. Applied Surface Science 280: 799-805.
34. Zabel, R.A., Morrell, J.J., 1992: Wood microbiology. Decay and its preservation. Academic Press, London Pp 52-89.
35. Zhou, Y.H., Wang, K., Hu, D.B., 2018: Degradation features of archaeological wood surface to deep inside a case study on wooden boards of Marquis of Haihun's outer coffin. Wood Research 63(3): 419-430.

Yihang Zhou, Kai Wang*, Dongbo Hu
Peking University
School of Archaeology and Museology
Beijing
P.R. China
*Corresponding author: wangkai2004@pku.edu.cn

Xueqi Chen
Peking University
College of Urban and Environmental Sciences
Beijing
P.R. China